Polymer Bulletin 53, 413–424 (2005)
DOI 10.1007/s00289-005-0347-8

Polymer Bulletin

The Effect of Macromolecular Architecture on Functional Group Accessibility: Hydrogen Bonding in Blends Containing Phenolic Photoresist Polymers

Carl Lawrence Aronson (✉), Douglas Beloskur, Isaac S. Frampton, Justin McKie and Bryce Burland

Department of Science and Mathematics, Kettering University, Flint, Michigan 48504 USA
E-mail: caronson@kettering.edu; Fax: (810) 762-7979

Received: 5 September 2004 / Revised version: 20 January 2005 / Accepted: 27 January 2005
Published online: 11 February 2005 –

Summary

An investigation of phenolic functional group accessibility in linear poly(4-hydroxy styrene) (PHS) and novel, branched poly(4-hydroxystyrene) (PHS-B) is presented. The phase behavior and extent of hydrogen bonding in blends of PHS-B with complimentary Lewis base polymers are calculated from glass transition temperature (T_g) enhancements measured using differential scanning calorimetry (DSC) techniques. The fraction of PHS-B hydroxyls accessible for hydrogen bonding were compared to linear PHS chains and small molecular weight analogs to help establish a molecular architecture-functional group accessibility property relationship for use with dissolution inhibition in candidate microlithographic photoresist binders. Design approaches to macromolecular structure and architecture for tailored intermolecular interactions in phenolic systems are discussed with respect to the effects of local steric screening as well as an intriguing thermodynamic competition between *inter*- and *intra*-molecular hydrogen bonding *via* molecular mechanics modeling.

Introduction

The accessibility of polymer functional groups is a function of repeat unit chemical composition and connectivity as well as overall molecular weight, tacticity and macromolecular architecture [1-2]. The accessibility of polar polymer side-groups (*i.e.* groups pendant to the chain backbone) capable of hydrogen bonding can directly dictate both local and global chain conformation as well as macroscopic solubility. Nevertheless, prediction of polymer functional group accessibility and concomitant thermodynamic solubility cannot be based solely on repeat unit atomic composition and connectivity such as with small molecular weight organic molecules. Macromolecular hydrogen bonded complexes involving high molecular weight linear chains and complementary small molecular weight oligomers are important in both biological as well as synthetic polymer systems. Complexation may occur *via* hydrogen bonding, ionic, charge transfer or Van der Waals interactions [3-4]. For example, hydrogen bonding in double stranded polynucleotide-oligonucleotide complexes controls a critical helix-coil equilibrium in many biological systems [5-6]. Furthermore, due to the entropic effects of polymer chains, stable hydrogen bonded

macromolecular complexes can form even if the interaction energy *per* segment is relatively small unlike low molecular weight organic analogs. Random insertion of a relatively small amount of chemically interacting groups into a polymer chain can produce miscibility in synthetic copolymer systems. For example, when polystyrene (PS) is modified to randomly contain merely 4% of 4-hydroxystyrene comonomer units, the decrease in ΔG caused by the -OH:::O=C< hydrogen bonded specific interactions rendered the modified PS miscible with poly(methyl methacrylate) [7].

PHS is an amorphous linear chain capable of both *inter*- as well *as intra*-molecular hydrogen bonding *via* the pendant *para*-hydroxyl groups (Figure 1(a)). Furthermore, the phenolic *p*-hydroxyl group in PHS possesses dual capabilities as a potential hydrogen bond donor and acceptor. Nevertheless, PHS apparently lacks significant organized regions of *intra*-molecular hydrogen bonding whereas *inter*-molecular hydrogen bonding tends to dominate. PHS is the archetypical polymer unit used in current positive photoresist formulations for microlithographic applications at both wavelengths of 248 nm (DUV) [8-13] and 13.4 nm (EUV) [14-15]. Branched poly(4-hydroxystyrene) (Figure 1(b)) is patented [16-17] and uniquely produced by DuPont® Electronic Polymers under the tradename PHS-B using carbocationic polycondensation copolymerization of 4-hydroxyphenylmethylcarbinol (4-HPMC) in the presence of oligomeric linear PHS [18]. The structure of PHS-B depicted in Figure 1(b) is a highly idealized schematic representation provided by DuPont® Electronic Polymers based on the ratio of 4-hydroxystyrene, *ortho-para* (di-substituted), *ortho-ortho-para* (tri-substituted) and end-group structures (Figure 2) determined from high resolution ^{13}C-NMR chemical shift data [16-18]. Nevertheless, PHS-B can be synthetically tailored to contain a certain quantity of linear PHS on average and its structure is intriguing due to the partial styrenic backbone character as well as phenol-acetaldehyde novolac-type branches as shown in Figure 1(b). Hence, the structure of PHS-B is effectively intermediate between linear PHS and a novolac resin. Furthermore, PHS-B can be synthetically tailored to possess a thermal resistance and dissolution rate in aqueous base that lies intermediate between linear PHS and conventional novolac binders [16-18]. In order for the phenolic resin binder to dissolve in aqueous base solution as desired, the OH^- ions from the solution must initially deprotonate a fraction of the *accessible* acidic phenolic pendant polymer sites [19].

It is hypothesized here that the accessibility of hydrogen bonding groups in PHS polymers is macromolecular architecture dependent and that this accessibility plays a key role in the primary functional chemistry governing their lithographic dissolution rate in aqueous base [20]. The degree of both *intra*- and *inter*-molecular hydrogen bonding among polymeric phenolic hydroxyl groups effectively governs their dissolution kinetics. As a result, we have turned our attention to the effect of PHS macromolecular architecture on functional group accessibility. Investigating the fraction of PHS-B hydroxyl groups accessible for hydrogen bonding and deprotonation compared to linear PHS would begin to establish a *critical molecular architecture-functional group accessibility property relationship* with respect to dissolution inhibition in PHS-based positive lithographic photoresist binders [8-15]. Wilson *et al.* [21] noted no increase in dissolution inhibition for comb poly(4-hydroxystyrene) possessing increasing degrees of branching and readily dismissed the effects of branching on the alkaline dissolution rate discrimination characteristics of phenolic polymer based photoresists. However, linear PHS, comb PHS and PHS-B do

not posses the same effective volume, steric hindrance or concomitant average pendant hydroxyl group accessibility. It is hypothesized that the periodic substitution *ortho* to the –OH group on the aromatic ring in PHS-B (Figure 1(b)) will substantially hinder accessibility. Furthermore, -OH groups located on terminal branches may have highly different accessibility on average compared to phenolic hydroxyl groups on interior branches in *non*-linear PHS-B [2]. Linear poly(2-vinyl pyridine) (P2VP) (Figure 1(c)), a complimentary polymeric Lewis base, is used herein as a macromolecular probe for hydrogen bonding and its potential hydrogen bond with Lewis acidic PHS-type molecules is shown in Figure 1(d) below.

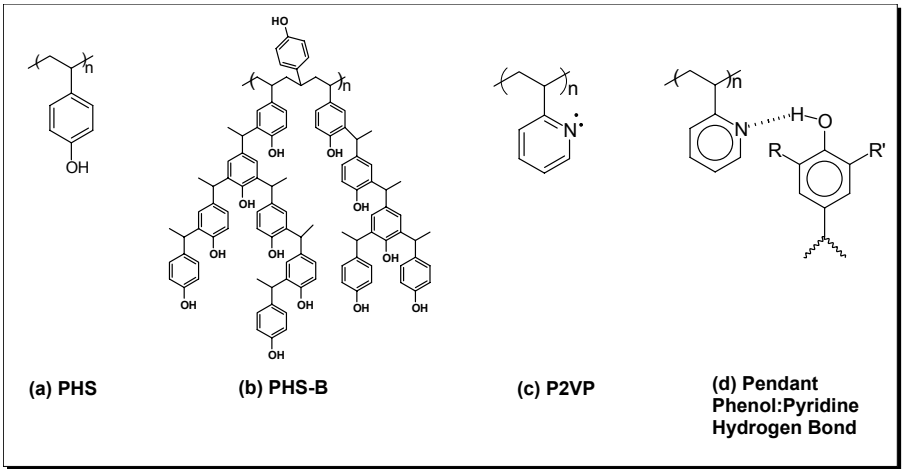

Figure 1. Chemical repeat structure of (a) linear poly(4-hydroxystyrene) (PHS), (b) branched poly(4-hydroxystyrene) (PHS-B), (c) linear poly(2-vinyl pyridine) (P2VP) and (d) *inter*-polymer hydrogen bonding interaction between pendant phenol and pyridine moieties.

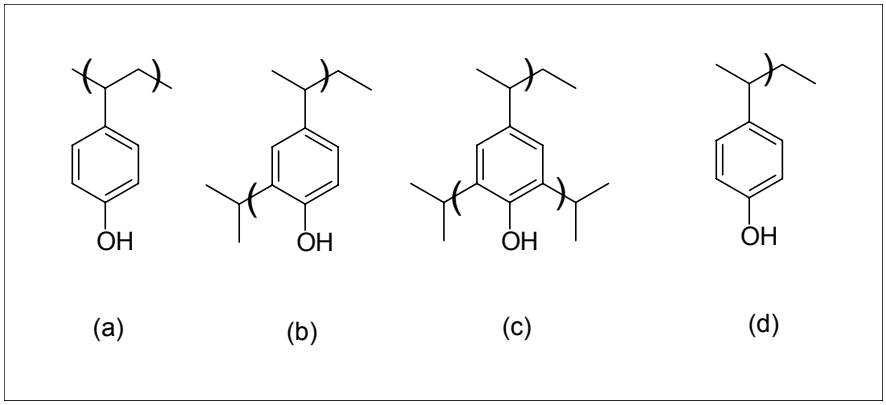

Figure 2. Chemical structures of the alkylation products obtained from the copolymerization of PHS with 4-HPMC to form PHS-B: (a) 4-hydroxystyrene, (b) di-substituted *ortho-para* alkylation, (c) tri-substituted *ortho-para* alkylation and (d) an end group.

Experimental

Materials

Reagent grade pyridine, tetrahydrofuran (THF) and methanol solvents as well as poly(2-vinyl pyridine) (P2VP, M_w=21,000 g/mole, degree of polymerization (DP) = 200; T_g = 92°C) were obtained from Aldrich Chemical Company (Milwaukee, WI) and used as received. Poly(4-hydroxy styrene) linear electronic grade (PHS; M_w = 8000, DP = 70; M_w/M_n = 2.24; T_g = 171°C) and poly(4-hydroxystyrene) branched grade (PHS-B; M_w = 4500; DP = 3; M_w/M_n = 1.84; T_g = 113°C) were donated by DuPont® Electronic Polymers (Dallas, TX) and used as received.

Thermal Analysis

Thermal analysis was conducted on a TA Instruments model 2920 Modulated Differential Scanning Calorimeter (DSC) using a heating rate of 20°C/minute under N_2 (g). All DSC samples were equilibrated at 60°C, heated to 280°C and held isothermally at 280°C for 1 minute. DSC cooling was accomplished using air. All polymer samples were cycled (heat-cool) at least three times and the glass transition temperatures (T_g) were determined from the third heating (unless otherwise stated) using the mid-point at half height between the transition's extrapolated onset and endpoint.

Infrared Spectroscopy

All infrared spectra were recorded on either a Thermo Nicolet® Avatar 360 E.S.P. or Nicolet® Impact 400 Fourier transform infrared (FT-IR) spectrometer operating at a resolution of 2 cm^{-1} in transmission using dried polymer samples crushed in KBr.

Nuclear Magnetic Resonance

High resolution ^{1}H- and ^{13}C-NMR spectra of 30 wt% polymer solutions in either acetone-d_6 or DMSO–d_6 solvent were recorded on a 500 MHz Varian FT-NMR spectrometer operating at 21°C using at least 128 and 4000 transients respectively.

Elemental Analysis

Elemental analyses for carbon (C), hydrogen (H) and nitrogen (N) were done in the microanalytical laboratory of the Department of Chemistry at Michigan State University, East Lansing.

Molecular Mechanics Modeling

Molecular mechanics energy minimization was accomplished using either PC Spartan Pro® (Wavefunction, Inc., Irvine, CA), version 2.0 with a molecular mechanics force field (MMFF94) or CaChe® (Fujitsu Ltd., Chiba City, Japan) version 3.2 with a molecular mechanics force field (MM2) [22].

Polymer Blends

Polymer blend solutions were synthesized by adding 3% (wt/vol) pyridine *homo*solvent solutions together. In general, no precipitation was observed for PHS/P2VP and PHS-B/P2VP polymer complexes upon addition of pyridine homosolvent solutions. After stirring magnetically, the polymer blend solutions in pyridine were poured onto an evaporation dish and allowed to stand overnight at room temperature in air. The solvent slowly evaporated in a fume hood. Evaporated blend films were subsequently dried *in vacuuo*.

Polymer Complexes

Polymer complexes were cast from either 3% (wt/vol) THF or 3% (wt/vol) methanol (MeOH) *homo*solvent solutions at room temperature. Polymer complex precipitates from THF or MeOH were isolated by decanting the supernatant followed by filtration. In all cases, the resulting solid polymer complex precipitate was dried initially in air and subsequently *in vacuuo* to form an optically clear, golden yellow film. PHS/P2VP and PHS-B/P2VP polymer complexes were observed to precipitate immediately upon addition of complimentary homopolymers dissolved in either THF or methanol *homo*solvent. The resulting vacuum dried polymer precipitate consistently formed a nearly 1:1 stoichiometric complex despite varying the polymer feed ratio between 10 and 90 wt% P2VP as characterized using ^{1}H-NMR (DMSO-d_6) and CHN elemental analysis. For example, *theoretical* 1:1 PHS-B ($C_{78}H_{108}O_{13}$)/P2VP (C_7H_7N): C, 77.35%; H, 7.70%; N, 6.66%; *experimental* precipitate recovered from 40/60 (wt/wt)% PHS-B/P2VP feed in methanol: C, 77.34%; H, 7.29%; N, 6.82%.

Results and Discussion

The glass transition temperature recorded for the 1:1 mole ratio PHS/P2VP and PHS-B/P2VP complexes cast from either *homo*THF or *homo*MeOH solutions was higher in general compared to 50/50 (wt/wt)% blends of the same polymers evaporated from pyridine solutions [23-25] indicating a higher degree of hydrogen bonding. Hence, although THF and methanol are polar solvents, these molecules were not observed to significantly compete with polymer-polymer hydrogen bonded association within either the PHS/P2VP or PHS-B/P2VP system and led to efficiently hydrogen bonded complexes. Conversely, polymer blends prepared by dissolving both components in pyridine did not immediately precipitate and tended to form optically clear films upon slow evaporation of the solvent at room temperature and atmospheric pressure with final drying *in vacuuo* following the work of Kato and Frechet [26-28]. Hence, in all cases the composition of the solid blend isolated from pyridine solutions was virtually identical to the initial polymer feed ratio from both ^{1}H-NMR (DMSO-d_6) and CHN elemental analysis. Pyridine solvent was able to effectively interact with the hydrogen bonding moieties of the PHS/P2VP and PHS-B/P2VP mixtures. Use of pyridine solvent also avoided premature formation of *inter*-polymer hydrogen bonds, which might interfere with blend equilibrium. A very broad infrared absorption centered around 3445 cm^{-1} corresponding to the O-H stretch (*intra*-molecular hydrogen bonding) was noted for neat PHS-B. Furthermore, a shift of the O-H stretch to a significantly lower vibrational frequency, centered around 3120 cm^{-1}, was noted upon introduction of 50 wt% P2VP into the system due to *inter*-polymer hydrogen bonding (-OH:::N) as portrayed in Figure 1(d). Optical transparency of the dried blend film as

well as electron microscopic homogeneity can be used to discern miscibility. Nevertheless, the most widely used criterion for establishing the miscibility of components in a polymer blend is the detection of a single glass transition temperature (T_g) usually at a point between the glass transition temperatures of the constituent polymers ($T_{g,a}$ and $T_{g,b}$). In contrast, thermodynamic phase separation is conventionally indicated when two separate glass transitions are observed for polymer blends.

In systems with specific *intra*- and/or *inter*-molecular interactions, such as hydrogen bonding, strong positive deviations from the linear composition dependence of T_g are commonly observed [7]. The empirical equation reported by Kwei *et al.* [29-30] shown in equation (1) below has been used to accurately model the T_g of hydrogen bonded binary (a-b) polymer blends with respective polymer weight fractions, w_a and w_b:

$$T_g = \{(w_a T_{g,a} + K w_b T_{g,b}) / (w_a + K w_b)\} + q w_a w_b. \quad (1)$$

In the Kwei equation (1) above, K and q are empirical constants and the product term ($q w_a w_b$) represents the number of hydrogen bonded specific interactions present in the mixture [31]. The term ($q w_a w_b$) also represents the excess average backbone stabilization energy imparted to the system due to hydrogen bonding. Despite the molecular formula of the PHS-B repeat unit (Figure 2) on average being similar to PHS (C_8H_8O), the two polymers are not precisely macromolecular isomers. Hence, absolute comparison of hydroxyl group functional group accessibility in PHS versus PHS-B must be made with some caution. Nevertheless, hydrogen bond efficiency for PHS-B with P2VP was compared to linear PHS here using DSC techniques in order to estimate the effect of polymer branching. It should be noted that the pyridine:phenol hydrogen bond enthalpy is significantly larger than the ΔH for phenol:phenol hydrogen bonded self-association [7]. Typical DSC thermograms for two different PHS-B/P2VP blend feed ratios isolated from pyridine are shown in Figure 3.

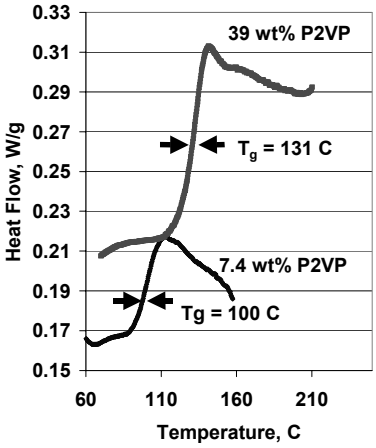

Figure 3. DSC thermograms (3rd heating cycle at a heating rate of 20°C/minute) for two different PHS-B/P2VP blends (a) 7.4 wt% P2VP in feed (single $T_{g,blend}$ = 100°C) and (b) 39 wt% (single $T_{g,blend}$ = 131°C) P2VP in feed isolated from pyridine.

A single glass transition was observed for all PHS and PHS-B blends with P2VP as isolated from pyridine. Thermal analysis of the PHS/P2VP and PHS-B/P2VP blends isolated from 3% pyridine solutions is summarized in Figure 4 with the corresponding Kwei *q* parameter [29-31] for each system determined from equation (1).

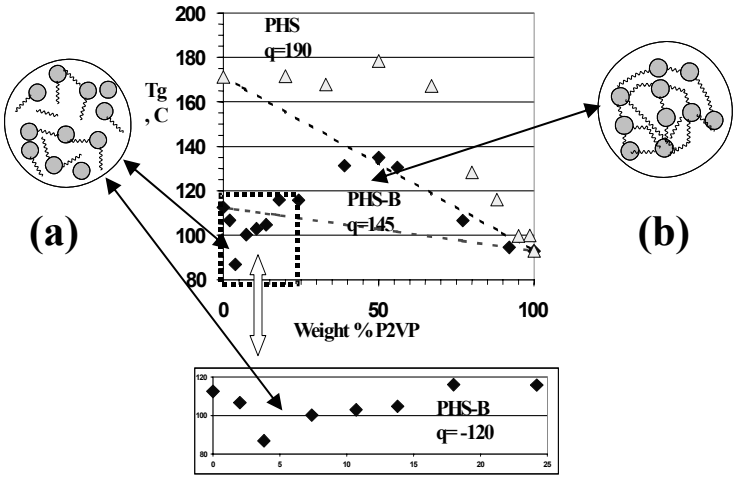

Figure 4. DSC thermal analysis of both PHS/P2VP and PHS-B/P2VP blends isolated from pyridine on 3rd heating cycle at a heating rate of 20°C/minute with accompanying idealized drawings of spherical PHS-B with linear P2VP in blends with hydrogen bonding capability.

For the PHS/P2VP blend system isolated from pyridine (Figure 4), where the Kwei [29-30] parameters $K = 1$ and $q > 0$, strong side-chain hydrogen bonding existed. A single glass transition as well as miscibility were observed over the entire composition range similar to other literature references for vinyl pyridine-vinyl phenol polymer blend systems [32-33]. For the PHS/P2VP system the maximum hydrogen bonded backbone stabilization energy ($R\ q\ w_a\ w_b$) was equal to 0.1 kcal/mole whereas the maximum overall backbone stabilization, represented by the product ($R\ T_g$), was equal to 0.9 kcal/mole where R is the gas constant (1.987 cal/K mole). The hydrogen bonding stabilization was equal to merely 10% of the overall energy and hence T_g was particularly sensitive to changes in backbone stabilization energy in the PHS/P2VP blend system.

When the concentration of the relatively long, linear P2VP chains was less than 25 wt%, the relatively short, spherical PHS-B molecules were in stoichiometric excess and were not observed to effectively serve as physical crosslink junction sites. Within this composition region (expanded in Figure 4 as region (a)) the linear P2VP chains were stoichiometrically limiting and simply inefficiently bonded to PHS-B creating *non*-hydrogen bonded (*i.e.* free) P2VP chain loops as well as both *non*-interacting trains and tail segments that effectively plasticized the system [34]. Furthermore, for the PHS-B/P2VP blend system within the P2VP<25 wt% composition region, limiting reagent P2VP chains were proposed to potentially wander within the spherical PHS-B molecule, solvate the globule and expand the equilibrium PHS-B conformation [35]. Diffusion and solvation of PHS-B by P2VP would significantly increase the overall *free volume* of the system and lower the macroscopically observed T_g.

Conversely, for concentrations above 25 wt% P2VP in the PHS-B/P2VP system the dispersed and continuum phases apparently switched as an inflection point was observed in the T_g versus concentration curve shown within Figure 4 region (b). Within this particular concentration region, strong side-chain hydrogen bonding produced backbone stabilization and significantly increased the T_g. Stoichiometrically limiting PHS-B served effectively as physical crosslink junction points and excess reagent linear P2VP chains served as macromolecular ties within an efficient physically crosslinked network *via inter*-molecular (*i.e.* inter-polymer) hydrogen bonds. Energy minimization of the isolated PHS-B structure using molecular mechanics modeling revealed a relatively dense, spherical globule whereby the phenolic moieties within the PHS-B interior were particularly sterically *screened* compared to the relatively *unhindered* phenolic moieties in linear PHS oligomers as shown in Figure 5 [2]. The planar phenyl rings were consistently observed to align vertically in a "napkin holder" type effect within the energy minimized PHS oligomeric structure as shown in Figure 5(a). Conversely, the planar phenyl rings were not observed to align vertically with respect to one another for energy minimized PHS-B as shown in Figure 5(b).

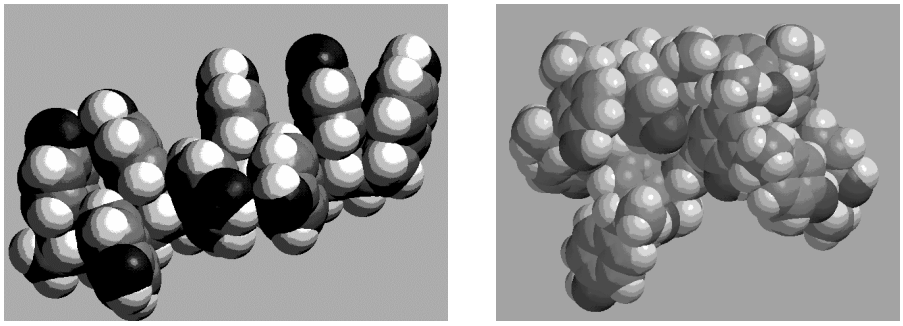

(a) PHS **(b) PHS-B**

Figure 5. Molecular mechanics (MM2 force field [22]) energy minimized CPK space-filling structures for (a) PHS octamer and (b) PHS-B repeat unit with Van der Waals contact distances for sphere radii (PC Spartan Pro®).

The molecular mechanics (MM2 force field) energy minimized structure of the entire PHS-B (degree of polymerization = 3, molecular weight = 4.7×10^3 g/mole) oligomer is shown in Figure 6. *Intra*-molecularly hydrogen bonded branch substructures were observed in the PHS-B molecular model leading to apparently higher order, organized hydrophilic channels due primarily to pendant group freedom. Furthermore, within the same energy minimized PHS-B molecule, formation of *intra*-molecular branch substructures were observed to be inhibited in some cases due to steric hindrance as well as stereochemical chiral (R,S) configuration of the tertiary (3°) carbon connecting between phenyl groups. In addition, local connectivity and global molecular architecture also appeared to affect substructure formation. Hydrophilic channel formation (Figure 6) was hypothesized to potentially facilitate movement of small metal countercations through the gradually deprotonated phenolate network in the case of alkaline dissolution for microlithographic photoresist applications [18-19].
The phenolic moieties were proposed to be sterically screened in PHS-B relative to linear PHS effectively creating an "inner harbor" effect. A two-dimensional

representation of the "inner harbor" effect is illustrated in Figure 7. For PHS-B the Lewis basic P2VP chain must apparently navigate a relatively narrow, sterically hindered and energetically challenging passage in order to hydrogen bond with interior branch phenolic hydroxyl groups [2].

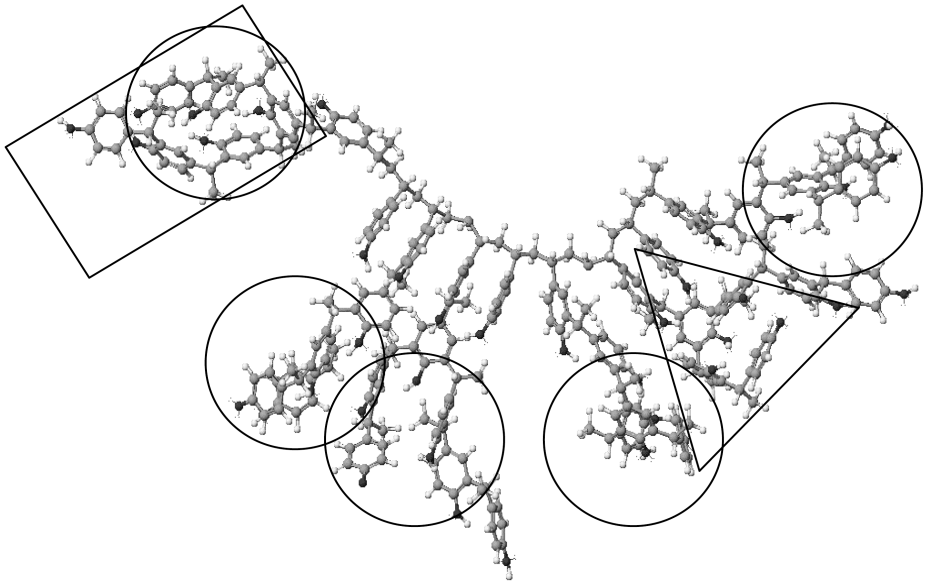

Figure 6. Ball-and-Spoke model of the PHS-B oligomeric structure (M_w=4680 g/mole) that was energy minimized using a molecular mechanics (MM2) force field (Cache® v. 3.2). Substructure formation (circle, O), unformed substructure due to steric hindrance (triangle, ∇) and organized hydrophilic channel caused by pendant group freedom (rectangle, □) are denoted.

Blends containing PHS-B (q = 145) had a Kwei q parameter that was 76% of blends containing linear PHS (q = 190) when each was mixed with 21,000 g/mole P2VP and isolated from pyridine solution over the entire composition range (Figure 4). Hence, PHS-B was considered to hydrogen bond with P2VP approximately ¾ as efficiently as linear PHS. The *inter*-molecular hydrogen bonding efficiency of partially hindered *ortho-para* (di-substituted) as well as fully hindered *ortho-ortho-para* (tri-substituted) small molecular weight phenol molecules has been reported [36-39]. Empirical modeling with hydrogen bond indices [36-39] derived from infrared absorption shifts [$\Delta\nu$ (cm^{-1})] for -OH groups of small molecular weight phenolic analogs was done here merely to compare with the effects of macromolecular connectivity and branching in the PHS-B macromolecule. *Un*hindered 4-*sec*-butyl phenol (1); *partially* hindered 2,4-*sec*-butyl phenol (2) and *fully* hindered 2,4,6-*sec*-butyl phenol (3) had normalized hydrogen bond indices of 1.00 (I_1), 0.693 (I_2) and 0.318 (I_3) respectively [37].
Analysis of the PHS-B repeat structure shown in Figure 1(b) indicates 5 sterically *un*hindered hydroxyl groups (n_1=5), 6 *ortho*-substituted *partially* hindered hydroxyls (n_2=6) and 2 *fully* hindered *ortho,ortho*-disubstituted phenolic hydroxyl groups (n_3=2) on average as denoted in Figure 8.

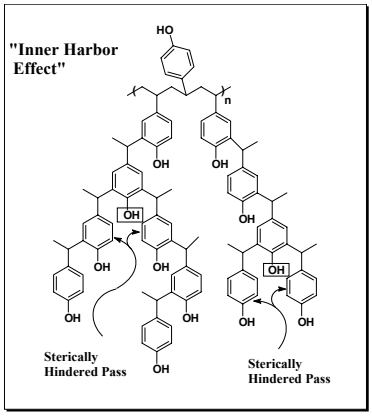

Figure 7. Sterically hindered pass and concomitant "inner harbor" effect for PHS-B.

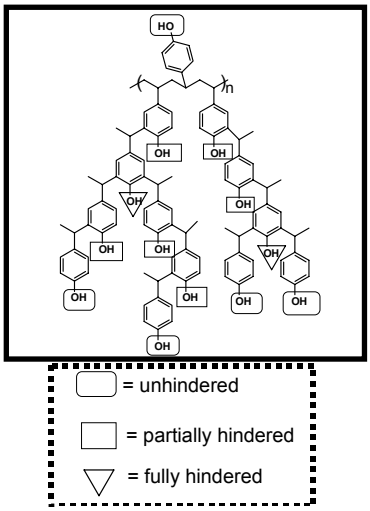

Figure 8. Empirical modeling with hydrogen bond indices for branched poly(4-hydroxy styrene) (PHS-B).

For PHS-B the simple sum of the product $[\Sigma(n_I \bullet I_i)]$ where i = 1-3 was 75% of the value calculated for linear PHS, which was comparable to the difference between the two molecules detected experimentally *via* thermal analysis. The PHS-B structure shown in Figure 8 is idealized from ^{13}C-NMR data as noted hereinabove [16-18]. In addition, the hydrogen bond indices for the small molecular weight analogs [36-39] certainly do not capture the complex conformations and stereochemical interplay required to satisfy equilibrium hydrogen bonding geometry of pendant phenolic hydroxyl moieties in coiled amorphous PHS and PHS-B chains. Nevertheless, the weighted sum of the hydrogen bond indices for small molecular weight hindered phenols, as determined simply from chemical repeat structure, was in close agreement with the Kwei T_g model for PHS-B in this particular case. Hence, preliminarily the local steric effects of aromatic substitution appear greater than the more global effects of macromolecular branching/conformation in PHS-B.

Despite the molecular formula of the PHS and PHS-B repeat units being similar, the two polymers are not precisely macromolecular isomers and absolute comparison of hydroxyl group accessibility must be made with thoughtful attention. Nevertheless, thermal analysis of hydrogen bonded *inter*-polymer blends containing either PHS or PHS-B as well as molecular mechanics modeling of both polymers indicate that tailored intermolecular interactions appear to be plausible by simply adjusting the [PHS]/[4-HPMC] feed concentration ratio in the acid-catalyzed PHS-B synthesis [16-18]. It is hypothesized that gradually increasing the concentration of linear PHS within the PHS-B structure will tend to increase *inter*-molecular hydrogen bonding, decrease *intra*-molecular hydrogen bonding and lower the overall steric hindrance local to the phenolic hydroxyl moieities. In contrast, increasing the concentration of 4-HPMC in the PHS-B macromolecular synthesis (*i.e.* increasing the branching and *ortho*-substitution polymer content) would tend to decrease *inter*-molecular hydrogen bonding but substantially increase *intra*-molecular hydrogen bonding. Increasing the [4-HPMC] is also hypothesized to increase the overall steric hindrance/local screening of the phenolic hydroxyl moieities theoretically reducing the alkaline dissolution rate [2, 20].

Conclusions

Unlike homogeneous and miscible PHS/P2VP blends, the PHS-B/P2VP blend system was observed to potentially *microphase* separate but remain compatible with unconventional Kwei thermal analysis parameters $K \neq 1$ and either a positive or negative value of q within two different composition regimes. The accessibility of the hydroxyl groups and average hydrogen bonding capacity of linear PHS was observed to be considerably higher than PHS-B prospectively due to both local steric (*i.e.* aromatic *ortho*-substitution) as well as global macromolecular architecture (*i.e.* globule conformation and branching) effects as observed from molecular mechanics modeling. The accessibility of phenolic hydroxyl groups was observed to significantly affect hydrogen bonding capacity and presumably would affect the ultimate dissolution rate of microlithographic PHS-containing photoresists. Hence, further investigation of the interplay between local and global steric effects in poly(4-hydroxystyrene) architectures appears highly worthwhile.

In an effort to further assess the effects of PHS molecular architecture, our laboratory is currently synthesizing a series of PHS-B molecules with varying degrees of branching or branching ratios (g) at relatively constant overall molar mass (M) by varying the [PHS]/[4-HPMC] copolymerization feed ratio. Characterization of the degree of branching, a ratio of the mean square radius of the branched polymer to the linear polymer ($g_M=\{\langle r^2_g\rangle_{branched}/\langle r^2_g\rangle_{linear}\}_M$) at constant M, is being carried out using size exclusion chromatography-multiangle laser light scattering (SEC-MALLS) techniques.

Acknowledgements. The authors wish to thank DuPont® Electronic Polymers (Dallas, TX) for the generous donation of PHS, PHS-B and 4-HPMC materials for this research. The authors also wish to thank the chemical staff at DuPont® Electronic Polymers (Ingleside, TX) as well as Dr. Dale J. Meier (Michigan Molecular Institute, Midland), Dr. Matthew Tirrell (University of California, Santa Barbara) and Dr. Charles R. Szmanda (Rohm and Haas Electronic Materials, Marlborough, Massachusetts) for their helpful discussions regarding this research.

References

1. Hsu WP, Yeh CF (1999) J Appl Polym Sci, 73: 431
2. Pruthikul R, Coleman MM, Painter PC, Tan NB (2001) J Polym Sci, Polym Phys, 39(14): 1651
3. Wang, LF, Pearce EM, Kwei TK, (1991) J Polym Sci, Polym Phys, 29, 619
4. Orfanou K, Topouza D, Sakellariou, G, Pispas S (2003) J Polym Sci, Polym Chem 41(16):2454
5. Magee WS, Gibbs JH, Zimm BH (1963) Biopolymers 1:133
6. Blake RD, (1972) Biopolymers 11:913
7. Coleman MM, Graf JF, Painter PC (1991) Specific Interactions and the Miscibility of Polymer Blends: Practical guides for Predicting and Designing Miscible Polymer Mixtures. Technomic, Lancaster PA
8. Ito H (2003) J Polym Sci, Polym Chem 41(24):3863
9. Ito H (2000) IBM J Res Dev 44:119
10. Ito H (1997) IBM J Res Dev 41:69
11. Ito H, Miller DC (2004) J Polym Sci, Polym Chem 42(6):1468
12. Ito H, Okazaki M, Miller DC (2004) J Polym Sci, Polym Chem 42(6):1478
13. Ito H, Okazaki M, Miller DC (2004) J Polym Sci, Polym Chem 42(6):1506
14. Cutler CA, Mackevich JF, Li J, O'Connell DJ, Cardinale GF, Brainard, RL (2003) SPIE 5037:40
15. Brainard RL, Cobb J, Cutler CA (2003) J Photopolymer Sci Tech 16(3):401
16. Sounik J, (1996) U.S. Patent Number 5,554,719
17. Sounik J, (1996) U.S. Patent Number 5,565,544
18. Sounik J, Vicari R, Lu PH, Kokinda E, Ficner S, Dammel, RR (1996) SPIE Advances in Resist Technology and Processing XIII, 2724:196
19. Ito H, IBM J Res Dev (2001) 45(5):683
20. Garza CM, Szmanda CR (1988) SPIE Proc 920:321
21. Wilson, CG, McAdams CL, Yueh W, Osborn, BP (2000) Am Chem Soc Polym Prep 41(1): 946
22. Allinger NL (1977) J Am Chem Soc 99:8127
23. Zeng XM, Chan CM, Weng LT, Li L (2000) Polymer 41:8321
24. Dai J, Goh SH, Lee SY, Siow KS Polym. J., 26, 905 (1994)
25. Zhou X, Goh SH, Lee SY, Tan KL (1997) Appl Surf Sci 119: 60
26. Kato T, Frechet, JMJ (1989) Macromolecules 22(9):3818
27. Kato T, Kihara H, Kumar U, Uryu T, Frechet JMJ (1994) Angew Chem Int Ed Engl 33: 1644
28. Frechet JMJ (2002) Proc Nat Acad Sci USA 99(8):4782
29. Kwei TK, (1984) J Polym Sci, Polym Lett 22:307
30. Lin AA, Kwei TK, Reiser A, (1989) Macromolecules, 22:4112
31. Georget DMR, Smith AC, Waldron KW (1999) Thermochimca Acta, 332:203
32. Lee JY, Moskala EJ, Painter PC, Coleman MM (1986) Appl Spectrosc, 40(7): 991
33. Meftahi MVD, Frechet JMJ. (1988) Polymer 29:477
34. Scranton AB, Klier J, Peppas NA (1991) J Polym Sci, Polym Phys Ed 29(2):211
35. Jeong M, Mackay ME, Vestberg R, Hawker CJ (2001) Macromolecules 34(14):4927
36. Puttnam NA (1960) J Chem Soc 2934
37. Puttnam NA (1960) J Chem Soc 486
38. Puttnam NA (1960) J Chem Soc 5100
39. Davis, MM (1968) Acid-Base Behavior in Aprotic Organic Solvents, Monograph 105, US National Bureau of Standards, Washington DC pp 25-30